Identification and functional characterization of eight CYP3A4 protein variants, Pharmacogenetics 11 (2001) 447–458.

[9] D. Dai, J. Tang, R. Rose, E. Hodgson, R.J. Bienstock, H.W. Mohrenweiser, J.A. Goldstein, Identification of variants of CYP3A4 and characterization of their abilities to metabolize testosterone and chlorpyrifos, J. Pharmacol. Exp. Ther. 299 (2001) 825–831.

[10] P. Villani, M. Pregnolato, S. Banfo, M. Rettani, D. Burroni, E. Seminari, R. Maserati, M.B. Regazzi, High-performance liquid chromatography method for analyzing the antiretroviral agent efavirenz in human plasma, Ther. Drug Monit. 21 (1999) 346–350.

[11] H.J. Xie, U. Yasar, S. Lundgren, L. Griskevicius, Y. Terelius, M. Hassan, A. Rane, Role of polymorphic human CYP2B6 in cyclophosphamide bioactivation, Pharmacogenomics J. 3 (2003) 53–61.

Available online at www.sciencedirect.com

SCIENCE DIRECT

Virology 327 (2004) 215–224

VIROLOGY

www.elsevier.com/locate/yviro

Novel patterns of nevirapine resistance-associated mutations of human immunodeficiency virus type 1 in treatment-naïve patients

Atsuko Hachiya[a], Hiroyuki Gatanaga[a,*], Eiichi Kodama[b], Mieko Ikeuchi[b], Masao Matsuoka[b], Shigeyoshi Harada[c], Hiroaki Mitsuya[c], Satoshi Kimura[a], Shinichi Oka[a]

[a]*AIDS Clinical Center, International Medical Center of Japan, Tokyo, Japan*
[b]*Institute for Virus Research, Kyoto University, Kyoto, Japan*
[c]*Department of Internal Medicine II, School of Medicine, Kumamoto University, Kumamoto, Japan*

Received 27 April 2004; accepted 2 July 2004
Available online 9 August 2004

Abstract

Several reports have recently shown that drug-resistant human immunodeficiency virus type 1 (HIV-1) is often isolated from treatment-naïve patients. We phenotypically analyzed HIV-1 strains isolated from 44 treatment-naïve individuals and found two strains highly resistant (69- and >310-fold) against nevirapine (NVP). Direct sequencing showed these two isolates had a novel mutation, K238S, in reverse transcriptase (RT), but did not have any reported NVP resistance-associated mutation.

A 48-h culture in the presence of NVP, however, selected HIV-1 carrying NVP resistance-associated mutations, V106A, V108I, or both, suggesting that minor viral populations of these two isolates had harbored these mutations. Replication kinetic studies of recombinant HIV-1 clones suggested that K238S conferred a significant resistance against NVP, especially when accompanied with V106A (530-fold) or V108I (56-fold). Our study identified a novel NVP resistance-associated mutation, K238S, which could be persistently detected by genotypic assay longer than V106A and V108I during off-treatment period.

Keywords: Human immunodeficiency virus type 1; K238S; Drug-naïve; Nevirapine-resistant

Introduction

The emergence of human immunodeficiency virus type 1 (HIV-1) variants resistant to antiretroviral agents is one of the most common causes for therapeutic failure in infected individuals. Fortunately, the availability of drug-resistance testing has substantially improved the ability of clinicians to deal knowledgeably with drug-resistant HIV-1 variants. Various guidelines for therapy of HIV-1 infection recommend that each individual therapy should be optimized by choosing efficient agents based on the results of drug-resistance testing. Numerous studies have recently reported that significant proportion of newly diagnosed HIV-1 infection cases are infected with viral strains resistant to at least one antiretroviral agent, justifying drug-resistance testing even in treatment-naïve patients (Briones et al., 2001; Duwe et al., 2001; Grant et al., 2002; Little et al., 2002; Salomon et al., 2000; Simon et al., 2002). However, it is important to recognize that the ability to detect resistant viruses may decrease as a function of time from initial infection because there is generally a shift to wild type over time during off-treatment (Devereux et al., 1999; Miller et al., 2000; Verhofstede et al., 1999). The usefulness of phenotypic assay could be enhanced if the virus is propagated in the presence of drug, because such a condition could propagate resistant viral strains that might have been outgrown by wild-type viruses in the absence of drug pressure. In this study, we screened 44 clinical strains isolated from newly infected individuals by using phenotypic assay and identified two highly nevirapine (NVP)-resistant isolates that could not be detected by genotypic

* Corresponding author. AIDS Clinical Center, International Medical Center of Japan, 1-21-1, Toyama, Shinjuku-ku, Tokyo 162-8655, Japan. Fax: +81 3 5273 5193.
E-mail address: higatana@imcj.acc.go.jp (H. Gatanaga).

0042-6822/$ - see front matter © 2004 Elsevier Inc. All rights reserved.
doi:10.1016/j.virol.2004.07.001

assay. Phylogenetic analyses showed these two isolates were genetically closely related and probably originated from a single patient. Furthermore, we identified a novel NVP resistance-associated mutation, K238S, in these isolates and determined its role in viral replication and resistance using newly generated recombinant HIV-1 clones.

Results

NVP-resistant HIV-1 from treatment-naïve patients

From January 2000 through December 2001, a total of 44 patients, who had had clinical evidence of recent HIV-1 infection (seroconversion or increased bands of western blotting against HIV-1 antigens), visited our clinic and all of them gave written informed consent to the participation in this study. To determine the prevalence of drug resistance in recent HIV-1 infection, susceptibility of HIV-1 isolates derived from these patients to six antiretroviral agents including zidovudine (AZT), lamivudine (3TC), stavudine (d4T), abacavir (ABC), NVP, and efavirenz (EFV) was examined phenotypically by using MAGIC-5 cells (CCR5 and CD4 expressing HeLa-LTR-β-gal cells) (Hachiya et al., 2001). As expected, most of such isolates were sensitive to all tested antiretroviral agents. However, two isolates (4.5%; isolated from Cases 33 and 23) showed significantly greater resistance (69-fold and more than 310-fold compared with NL4-3) to NVP, though their resistance to EFV was not high (Fig. 1, Table 1).

To delineate the mechanism of the NVP resistance in the above two isolates, direct sequencing of HIV-1 reverse transcriptase (RT) gene from plasma samples was performed. Both plasma-derived sequences did not have any non-nucleoside RT inhibitor (NNRTI) resistance-associated mutations listed in resistance table of the International AIDS Society (Johnson et al., 2003) but had six-amino-acid substitutions including V35I, R83K, I135T, T200K, R211K, and K238S, compared with HXBII sequences, and the plasma-derived sequence in Case 23 had a mixture of K102 and K102R (Table 2). We postulated that there might be a minor viral population harboring NNRTI resistance-associated mutations in both plasma samples, which could not be detected by direct sequencing. To detect such a minor NVP-resistant viral population, the clinical isolates were propagated in MAGIC-5 cells in the presence of NVP at various concentrations and the RT gene of HIV-1 obtained from a 48-h culture supernatant was analyzed. In the HIV-1 isolated from Case 33, V108I, known as a NVP resistance-associated mutation, emerged in the presence of NVP (1 μM) although it could not be detected in direct sequencing of plasma (Table 2). In the HIV-1 isolated from Case 23, V106A, and V108I emerged in the presence of NVP (1 and 10 μM). Interestingly, clonal sequencing analysis of HIV-1 culture (NVP 1 μM) isolated from Case 23 revealed that K102R and V106A always coexisted on the same molecules and that V108I did not coexist with K102R and V106A (Table 2). All clones analyzed had V35I, R83K, I135T, T200K, R211K, and K238S. Four of these mutations (V35I, R83K, I135T, and R211K) are known as polymorphic mutations and were frequently observed in HIV-1 isolated from treatment-naïve individuals in our cohort (72%, 18%, 27%, and 36%, respectively, $n = 11$). T200K and K238S had not been reported previously and might be associated with NVP resistance.

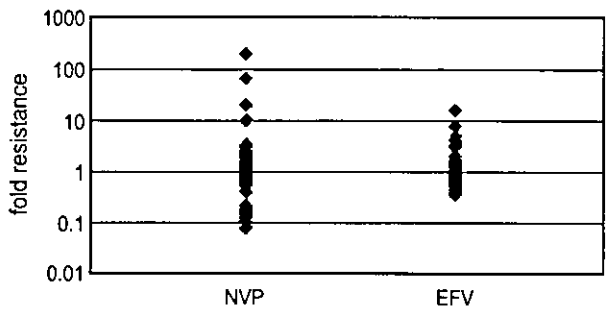

Fig. 1. Results of drug resistance assay using MAGIC-5 cells in treatment-naïve individuals. Fold resistances compared with NL4-3 are shown.

Phylogenetic analysis of clinical HIV-1 isolates

Because the clinical HIV-1 isolates derived from Cases 33 and 23 had unusually high resistance against NVP and had exactly the same amino acid substitutions (V35I, R83K, I135T, T200K, R211K, and K238S), we suspected that these two patients had acquired HIV-1 infection from a single infected patient. Then, we phylogenetically analyzed the direct sequences of *env* region and RT gene of the two HIV-1 isolates derived from Cases 33 and 23, and then compared their sequences with four clinical isolates derived from other patients (Cases 2, 3, 26, and 29) and five referential unrelated strains [U63632, HXB2CG, OY1, RF, and simian immunodeficiency virus (SIV)]. In both phylogenetic trees using the sequences of the *env* region and RT gene, Cases 33- and 23-derived sequences formed a tight cluster separated from other sequences by the tree branch with high bootstrap probabilities (99% and 100%) (Figs. 2A and B), suggesting that the isolates from Cases 33 and 23 were genetically closely related and probably originated from a single source. It was noteworthy that the *env* sequences derived from Cases 33 and 23 were closely related but not identical, which excludes the possibility of contamination during the procedures of viral culture and PCR.

Three-dimensional positions of mutations and NVP-binding pocket in HIV-1 RT

To delineate the positional relationship between NVP-binding pocket and the mutations in RT described above, a structural model of HIV-1 RT complexed with NVP was

Table 1
Results of phenotypic drug resistance testing in two untreated patients

HIV-1	IC_{50}[a] [μM] (fold resistance[b])					
	AZT	3TC	d4T	ABC	NVP	EFV
Case 33	0.04 ± 0.03 (1.2)	0.61 ± 0.20 (1.8)	1.7 ± 0.10 (0.77)	3.6 ± 0.87 (2.3)	2.2 ± 0.29 (69)	0.011 ± 0.003 (4.2)
Case 23	0.12 ± 0.03 (3.5)	0.81 ± 0.15 (2.4)	3.2 ± 0.95 (1.5)	3.3 ± 0.87 (2.1)	>10 (>310)	0.023 ± 0.00002 (8.8)

Data are mean ± SD. Numbers in parentheses represent fold resistance.
[a] Phenotypic drug resistance assay was performed using MAGIC-5 cells.
[b] Fold resistance was calculated by dividing IC_{50} of clinical isolate by that of NL4-3 (AZT, 0.034 μM; 3TC, 0.34 μM; d4T, 2.2 μM; ABC, 1.6 μM; NVP, 0.032 μM; EFV, 0.0026 μM).

prepared based on the published crystal structures (Fig. 3) (Ren et al., 2000). The Val residues at 106 and 108 codons of RT (V106 and V108), the site of NNRTI resistance-associated mutations, V106A and V108I, respectively, were in close contact with NVP, packed in the hydrophobic pocket of the palm domain. Five residues, V35, R83, I135, T200, and R211, were located distantly from the hydrophobic pocket. Two residues, K102 and K238, were located outside the frame of hydrophobic pocket and the substitutions of these amino acids, such as K102R and K238S, were thought to produce some structural changes of the pocket and might be associated with NNRTI resistance.

Role of K102R and K238S in HIV-1 replication and resistance against NVP

Because K238S has not been reported previously and K102 and K238 were located on the frame of NVP-binding pocket, we chose to construct seven recombinant HIV-1 strains, HIV-1_{K102R}, HIV-1_{V106A}, HIV-1_{V108I}, HIV-1_{K238S}, HIV-$1_{V106A/K238S}$, HIV-$1_{V108I/K238S}$, and HIV-$1_{K102R/V106A/K238S}$, to delineate the effects of K102R and K238S on viral susceptibility against NVP. K102R did not confer significant resistance against NVP and EFV (Table 3), while V106A and V108I, both of which were known as NVP resistance-associated mutations, conferred 97- and 3.8-fold resistance against NVP, respectively. However, these mutations did not confer significant resistance against EFV. K238S conferred a significant resistance against NVP as did V108I. Interestingly, the combination of V106A and K238S (V106A/K238S) conferred surprisingly high-level resistance (530-fold) against NVP, and the combination of V108I and K238S (V108I/K238S) also conferred high resistance (56-fold) only against NVP but not against EFV (Table 3). Furthermore, the triple combination of K102R, V106A, and K238S (K102R/V106A/K238S), which were found in 15 of 21 clones derived from Case 23 (Table 2), also conferred high resistance (340-fold) against NVP, although its effect on viral resistance against EFV was not significant (Table 3). These data suggest that K238S is strongly associated with NVP resistance in the combination with V106A or V108I.

We next analyzed the effects of K102R and K238S on viral replication kinetics in the absence or presence of NVP. The addition of K238S to HIV-1WT (HIV-1_{K238S}) reduced the replication of HIV-1_{WT} in the absence of NVP, and the addition of V108I to HIV-1_{K238S} (generating HIV-$1_{V108I/K238S}$) further reduced the viral replication (Fig. 4A). On the other hand, in the presence of NVP (1 μM), K238S made HIV-1 replication-competent (HIV-1_{WT} could not replicate), and HIV-$1_{V108I/K238S}$ had facilitated viral replication (Fig. 4B). The combination of V106A to K238S (HIV-$1_{V106A/K238S}$) severely compromised viral replication and the addition of K102R (HIV-$1_{K102R/V106A/K238S}$) did

Table 2
Sequences of HIV-1 RT-coding region of clinical samples and isolates

	Sequenced sample	Amino acid residue														
		35	83	100[a]	102	103[a]	106[a]	108[a]	135	181[a]	188[a]	190[a]	200	211	230[a]	238
HXBII		V	R	L	K	K	V	V	I	Y	Y	G	T	R	M	K
Case 33	plasma	I	K	–	–	–	–	–	T	–	–	–	K	K	–	S
	1 μM[b]	I	K	–	–	–	–	V/I	T	–	–	–	K	K	–	S
Case 23	plasma	I	K	–	K/R	–	–	–	T	–	–	–	K	K	–	S
	1 μM[b]	I	K	–	K/R	–	V/A	V/I	T	–	–	–	K	K	–	S
	10 μM[b]	I	K	–	K/R	–	A	V/I	T	–	–	–	K	K	–	S
	Number of clones															
Isolate from	15	I	K	–	R	–	A	–	T	–	–	–	K	K	–	S
Case 23	3	I	K	–	–	–	–	–	T	–	–	–	K	K	–	S
(1 μMb)	2	I	K	–	–	–	–	I	T	–	–	–	K	K	–	S
	1	I	K	–	–	R	–	–	T	–	–	–	K	K	–	S

Amino acids identical to HXBII (top column) are indicated with dashes.
[a] Reported residue associated with NVP resistance (Johnson et al., 2003).
[b] Cultured HIV-1 isolate in the presence of NVP at the indicated concentrations.

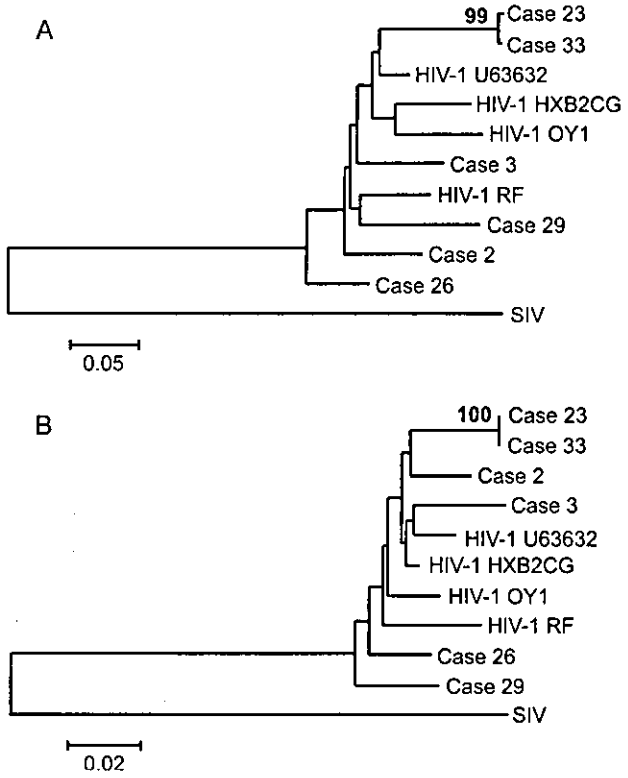

Fig. 2. Phylogenetic analysis of *env* sequences (A) and RT genes (B) of six clinical isolates and five referential strains. Bootstrap probabilities of important tree branches are shown as percentages.

not seem to rescue its replicability in the absence of drugs (Fig. 4C). In the presence of NVP (1 μM), the combination of V106A and K238S (HIV-$1_{V106A/K238S}$) rendered HIV-1 replicable, and the addition of K102R to V106A/K238S (HIV-$1_{K102R/V106A/K238S}$) did not significantly alter the replication (Fig. 4D). These data showed that V108I/K238S and V106A/K238S can confer viral replicability in the presence of NVP, although the role of K102R when combined with V106A/K238S remained to be determined.

Table 3
Drug resistance of recombinant HIV-1s

Recombinant HIV-1	IC_{50}[a] [μM] (fold resistance[b])	
	NVP	EFV
K102R	0.047 ± 0.02 (1.5)	0.002 ± 0.001 (0.77)
V106A	3.1 ± 0.36 (97)	0.002 ± 0.0003 (0.77)
V108I	0.12 ± 0.03 (3.8)	0.001 ± 0.0001 (0.38)
K238S	0.14 ± 0.04 (4.4)	0.002 ± 0.0003 (0.77)
V106A/K238S	17 ± 4.6 (530)	0.004 ± 0.001 (1.5)
V108I/K238S	1.8 ± 0.66 (56)	0.001 ± 0.0001 (0.38)
K102R/V106A/K238S	11 ± 3.1 (340)	0.002 ± 0.0001 (0.77)

Data are mean ± SD. Numbers in parentheses represent fold resistance.
[a] Phenotypic drug resistance assay was performed using MAGIC-5 cells.
[b] Fold resistance was calculated by dividing IC_{50} of clinical isolate by that of NL4-3 (NVP; 0.032 μM, EFV; 0.0026 μM).

To further define the significance of each mutation, the viral replicability was compared among molecular infectious HIV-1 clones described above in the presence and absence of NVP using competitive HIV-1 replication assay (CHRA) (Kosalaraksa et al., 1999). Two infectious HIV-1 clones to be compared for their fitness were mixed and used to infect H9 cells, and their population changes through passages were determined by the relative peak height on sequencing electrogram. In the absence of NVP, HIV-1_{WT} readily outgrew HIV-

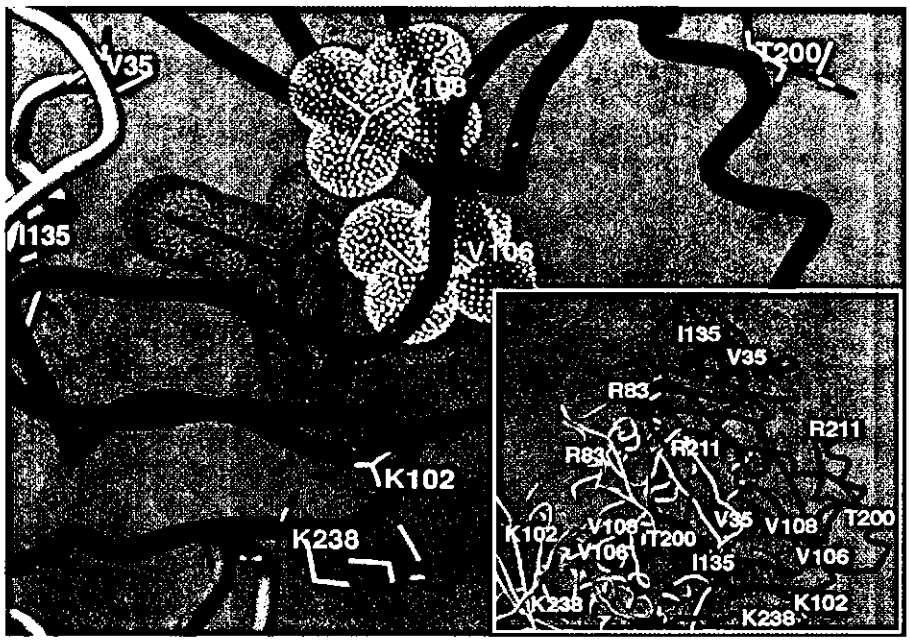

Fig. 3. The structure of the HIV-1 RT complexed with NVP. A view of the RT complexed with NVP, generated using SYBYL 6.7 and the coordinate set 1FKP.pdb obtained from the Protein Data Bank (Ren et al., 2000). The fingers, palm, thumb, and connection subdomains of the p66 subunit are colored blue, red, green, and yellow, respectively. The p51 subunit is colored white. Residues of the p66 subunit are yellow-colored, while those of the p51 subunit are white-colored. The van der Waals volumes of side chain of V106 and V108 (white) are shown to interact with NVP (orange).

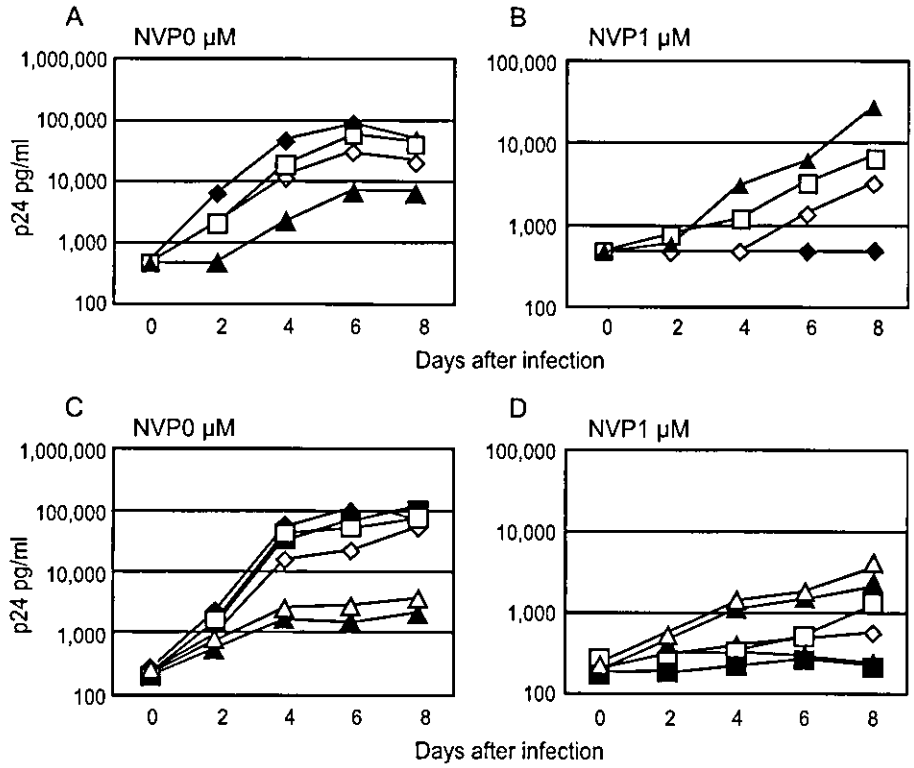

Fig. 4. Replication kinetics of recombinant HIV-1s. Graphs A and B show replication kinetics of HIV-1_{WT} (solid diamonds), HIV-1_{V108I} (open squares), HIV-1_{K238S} (open diamonds), and HIV-$1_{V108I/K238S}$ (solid triangles) in the absence and presence of NVP (1 μM), respectively. Graphs C and D show replication kinetics of HIV-1_{WT} (solid diamonds), HIV-1_{K102R} (solid squares), HIV-1_{V106A} (open squares), HIV-1_{K238S} (open diamonds), HIV-$1_{V106A/K238S}$ (solid triangles), and HIV-$1_{K102R/V106A/K238S}$ (open triangles) in the absence and presence of NVP (1 μM), respectively. The results shown are representative of three independent experiments.

1_{K238S} (Fig. 5A). In the presence of NVP (0.1 μM), however, HIV-1_{K238S} predominated over HIV-1_{WT} (Fig. 5B), suggesting that K238S compromised the viral replication in the absence of NVP but conferred resistance against NVP. Next, we analyzed the effect of V106A and V108I on HIV-1_{K238S} replication. In comparison between HIV-1_{K238S} and HIV-$1_{V106A/K238S}$, HIV-1_{K238S} predominated over HIV-$1V_{106A/K238S}$ in the absence of NVP (Fig. 5C), but was outgrown by HIV-$1_{V106A/K238S}$ in the presence of NVP (1 μM) (Fig. 5D). In comparison between HIV-1_{K238S} and HIV-$1_{V108I/K238S}$, HIV-1_{K238S} predominated over HIV-$1_{V108I/K238S}$ in the absence of NVP (Fig. 5E), but was outgrown by HIV-$1_{V108I/K238S}$ in the presence of NVP (1 μM) (Fig. 5F). Taken together, these data suggest that each of V106A and V108I compromised the viral replication in the absence of NVP but conferred resistance against NVP. Finally, we analyzed the effect of K102R on replication of HIV-1_{WT} and HIV-$1_{V106A/K238S}$. HIV-1_{K102R} was slowly overcome by HIV-1_{WT} in the absence of NVP (Fig. 5G). In comparison between HIV-$1_{V106A/K238S}$ and HIV-$1_{K102R/V106A/K238S}$, HIV-$1_{K102R/V106A/K238S}$ predominated over HIV-$1_{V106A/K238S}$ both in the absence (Fig. 5H) and presence (1 μM) (Fig. 5I) of NVP. Considered together, these results suggest that K102R compromised the replication of HIV-1_{WT} but compensated the replication ability of HIV-$1_{V106A/K238S}$ regardless of the presence of NVP.

Discussion

Several studies reported the recent spread of drug-resistant HIV-1 in the developed countries and among treatment-naïve individuals as well, which has been a menace for clinicians. Therefore, for certain treatment-naïve patients, such as cases of acute or recent HIV-1 infection, drug-resistance assay is recommended (Hirsch et al., 2003). However, resistant HIV-1 can be replaced with wild-type HIV-1 rapidly in plasma in the absence of treatment, and it may be difficult to detect resistant HIV-1 in the treatment-naïve patients even if they harbored resistant HIV-1. In this regard, phenotypic assay may be superior to genotypic assay using direct sequencing, because in phenotypic assay, resistant viruses could be propagated during culture in the presence of antiretroviral agents, while direct sequencing can only detect relatively major viral population in plasma. In fact, in the present study, the phenotypic assay using MAGIC-5 cells detected two highly NVP-resistant isolates in treatment-naïve patients, in whom direct sequencing failed to detect the presence of minor population of V106A and V108I.

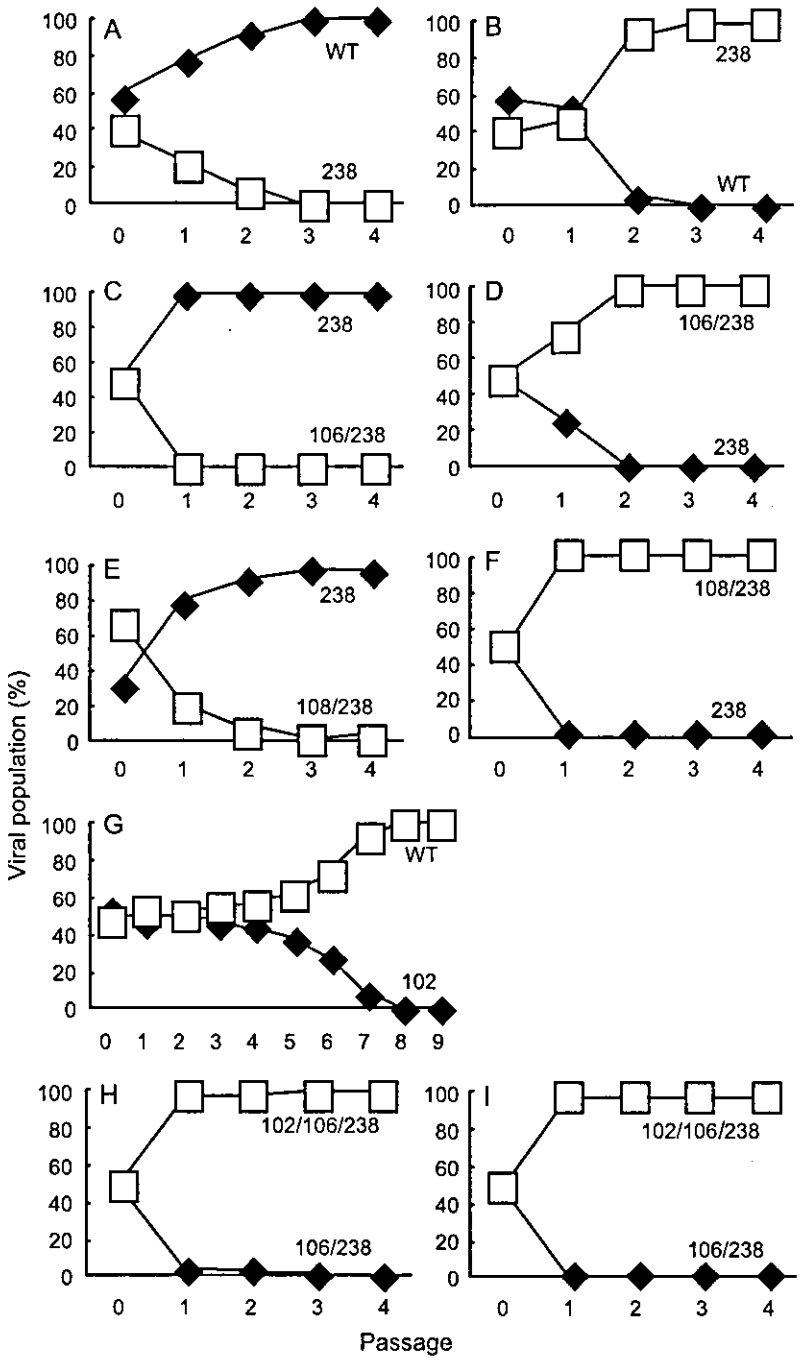

Fig. 5. Competitive HIV-1 replication assay for recombinant HIV-1s. Two infectious HIV-1 clones to be compared for their fitness were mixed and used to infect H9 cells in the absence (A, C, E, G, and H) and presence of NVP (B: 0.1 μM; D, F, and I: 1 μM). The cell-free supernatant was transferred to fresh H9 cells every 7 days. High-molecular-weight DNAs extracted from infected cells at the end of each passage were subjected to nucleotide sequencing, and proportion of Lys and Ser at position 238 (Graphs A and B), those of Val and Ala at position 106 (Graphs C and D), those of Val and Ile at position 108 (Graphs E and F), and those of Lys and Arg at position 102 (Graphs G–I) were determined.

The use of NVP has markedly increased worldwide because a single formulation of NVP combined with d4T and 3TC is a generic drug widely used in resource-limited situations (Cohen, 2003; Penzak et al., 2003). The use of NVP in pregnant women is also one of the main strategies to prevent mother-to-child transmission of HIV-1 (Guay et al., 1999; Marseille et al., 1999). Therefore, understanding of the mechanism of NVP resistance development is urgently needed.

In the present study, we identified a novel mutation, K238S, which was associated with a high multitude of NVP resistance when it was coupled with V106A or V108I. Interestingly, direct sequencing identified only K238S in the two patients infected with highly NVP-resistant HIV-1.

These results showed that V106A and V108I were reverting to their wild-type V106 and V108, respectively, in major viral populations in the plasma. Furthermore, the results indicate that K238S can remain longer than V106A and V108I in the absence of NVP treatment, partly because at least two nucleotide substitutions are required for K238S while V106A and V108I can occur with only a single nucleotide substitution.

M230 is located on the opposite side of Q151 in relation to the incoming dNTP, forming the primer grip of RT and contacting the primer strand (Huang et al., 1998; Sarafianos et al., 1999), and several mutations around this site were reported to occur in patients during NNRTI treatment. Parkin et al. (2000) observed the emergence of F227L and M230L during NVP-containing combination therapy and it was associated with the loss of NVP susceptibility of their clinical isolates. Demeter et al. (2000) reported that P236L occurred in subjects receiving delavirdine monotherapy. With regard to K238, Demeter et al. (1998) observed the emergence of K238T in one patient treated with atevirdine (an NNRTI) and AZT. Considering these reports, the region containing M230 and K238 is important for drug susceptibility and there may be more resistance-associated mutations around these sites.

Phylogenetic analysis showed a close relation between the isolates from Cases 33 and 23 (Fig. 2), suggesting that the two patients had acquired HIV-1 infection from the same source, although they did not know each other and interviewing them could not identify the source patient. This source patient presumably had been under antiretroviral treatment including NVP, which had failed to suppress his viral load because of the sets of mutations, K102R/V106A/K238S and V108I/K238S. It remains unknown whether K238S had existed as a polymorphism before the introduction of antiretroviral treatment, or it had emerged during NVP treatment in the source patient. Considering that a single dose of NVP to prevent mother-to-child transmission can induce resistant strains (Morris et al., 2003; Sullivan, 2003), some polymorphic mutations in treatment-naïve population could be associated with NVP resistance.

Materials and methods

Reagents and cells

AZT, d4T, and ABC were purchased from Sigma Co. (Tokyo, Japan). 3TC, NVP, and EFV were generously provided by Nippon Glaxo-Smithkline (Tokyo, Japan), Boehringer Ingelheim Pharmaceutics Inc. (Ridgefield, CT), and Merck Co. Inc. (Rahway, NJ), respectively.

H9 cells and COS-7 cells were grown in RPMI 1640 and Dulbecco's modified eagle medium (DMEM), respectively, supplemented with 10% fetal calf serum (FCS), penicillin (100 U/ml), and streptomycin (100 μg/ml). MAGIC-5 cells (CCR5 and CD4 expressing HeLa-LTR-β-gal cells) (Hachiya et al., 2001, 2003) were grown in DMEM supplemented with 10% FCS, hygromycin B (100 μg/ml) (Invitrogen Co., Carlsbad, CA), and blasticidin (1 μg/ml) (Funakoshi, Tokyo). Peripheral blood mononuclear cells (PBMCs) obtained from healthy donors were stimulated by phytohemagglutinin (PHA) in RPMI 1640-based medium containing interleukin-2 (20 U/ml) (R & D Systems, Minneapolis, MN) for 2 days before HIV-1 exposure.

Patients and clinical isolates

Clinical strains were isolated from fresh plasma of the study participants attending the outpatient clinic of the AIDS Clinical Center, International Medical Center of Japan, by using MAGIC-5 cells as described previously (Hachiya et al., 2001). The obtained isolates were stored at −80 °C until use and the infectivity was measured as blue cell-forming unit (BFU) of MAGIC-5 cells (Hachiya et al., 2001). The Institutional Review Board approved this study (IMCJ-H13-80) and a written informed consent was obtained from all the participants.

Case 33 was a 33-year-old homosexual man. He suffered from high fever and severe headache, probably symptoms of primary HIV-1 infection, in April 2000. On May 15, Western blotting showed faint bands against HIV-1 gp160, p68, p55, p25, and p18 antigens. One week after, these bands became bold and new bands against HIV-1 gp110, p40, and p34 antigens appeared. The CD4 count was 401/μl and HIV-1 viral load was 2.0×10^5/ml.

Case 23 was a 23-year-old homosexual man. He also suffered from severe headache and was hospitalized in January, 2001. Western blotting showed one faint band against HIV-1 gp160 antigen. In April, 2001, the band became bold and new bands against gp110, p68, p55, p52, gp41, p40, p34, p25, and p18 antigens appeared. The CD4 count was 210/μl and HIV-1 viral load was 7.1×10^4/ml.

Sequence analyses of HIV-1 RT and V3 region

Viral RNA was extracted from plasma and clinical isolates with Smi-test nucleic acid extraction kit (Genome Science, Fukushima, Japan). The HIV-1 RT gene was amplified by RT-PCR using One Step RNA PCR Kit (Takara Shuzo, Otsu, Japan). For plasma-derived RNA, nested PCR was conducted subsequently to amplify enough DNA for direct sequencing. The sequences of primer sets for the first PCR (T1 and T4) and the second PCR (T12 and T15) were as follows (Gatanaga et al., 1999; Hachiya et al., 2001, 2003): T1, 5′-AGGGGGAATTGGAGGTTT (RF positions, 1910 to 1927); T4, 5′-TTCTGTTAGTGCTTTGGTT (RF positions, 2939–2921); T12, 5′-CCAGTAAAATTAAAGCCAG (RF positions, 2091–2109); and T15, 5′-TCCCACTAACTTCTGTATGTC (RF positions, 2852–2832). The gp120 V3 domain of several HIV-1 isolates was amplified by RT-

PCR and nested PCR. The sequences of primer sets for the first PCR (ES1 and EA1) and the second PCR (ES2 and EA2) were as follows (Ida et al., 1997): ES1, 5′-AATGTCAGCACAGTACAATGTACAC (RF positions, 6502–6526); EA1, 5′-ACAATTTCTGGGTCCCCTCCTGAGGA (RF positions, 6890–6865); ES2, 5′-ATGGAATTAGGCCAGTAGTG (RF positions, 6527–6546); EA2, 5′-CTCCTAATTTTGTAACTAC (RF positions, 6829–6811). Specific precautions, including physical separation of processing areas, were taken to avoid template and amplified product carryover. Stringent quality control to prevent PCR contamination was employed to protect against cross-contamination of product DNA. Direct sequencing was performed using dye terminators (BigDye Terminator Cycle Sequencing Ready Reaction Kit; Applied Biosystems, Foster, CA) and model 3700 automated DNA sequencer (Applied Biosystems). Amino acid sequences were deduced with the Genetyx-Win program version 4.1 (Software Development, Tokyo). For some PCR products, molecular cloning was performed with pT7 Blue T-Vector (Novagen, CA) and their sequences were analyzed.

For the phylogenetic analysis, RT gene and V3 sequences were aligned by Clustal-W program with reference sequences from the Los Alamos sequence database. The results of the alignment were then analyzed by the neighbor-joining method and the distance matrixes were generated with Kimura two-parameter model.

Bootstrap resampling (1000 data sets) of the multiple alignments was performed to test the statistical robustness of the tree.

Construction of recombinant HIV-1 clones

Recombinant infectious HIV-1 clones carrying various mutations in RT were constructed with a site-directed mutagenesis. Briefly, the desired mutations were introduced into *Xma*I–*Nhe*I region (759 bp) of pTZNX1, which encoded Gly-15 to Ala-267 of HIV-1 RT (strain BH 10), by the oligonucleotide-based mutagenesis method (Kodama et al., 2001). The *Xma*I–*Nhe*I fragment was inserted into pNL101-based plasmid (a kind gift from Jeang Kuan-The, NIAID/NIH, Bethesda, MD), generating various molecular clones with the desired mutations. Determination of the nucleotide sequences of plasmids confirmed that each clone had the desired mutations but no unintended mutations. Each molecular clone (10 μg/ml as DNA) was transfected into COS-7 cells (4×10^5 cells/100-mm-diameter dish) by Fugene transfection reagent (Roche Diagnosis, Basal, Switzerland). After 48 h, culture supernatants were harvested and stored at −80 °C until use. The infectivity of the viruses was determined as BFU in MAGIC-5 cells.

Drug susceptibility assay with MAGIC-5 cells

HIV-1 drug susceptibility to various RTIs was determined in triplicate by using MAGIC-5 cells as described previously (Hachiya et al., 2001). Briefly, MAGIC-5 cells were infected with adjusted virus stock (300 BFU) in the presence of increasing concentrations of RTIs, cultured for 48 h, fixed, and stained with 5-bromo-4-chloro-3-indolyl-β-D-galactopyranoside (Takara Shuzo). The blue-stained cells were counted under a light microscope. Drug concentrations that inhibited 50% of the stained cells of drug-free control (IC_{50}) were determined by referring to the dose–response curve.

Viral replication kinetic assays

PHA-stimulated PBMCs were exposed to each infectious virus preparation (300 BFU) in a final volume of 200 μl for 2 h. Infected cells were then washed and cultured in a volume of 200 μl in the absence or presence of NVP (1 μM). Assays were performed in triplicate and repeated at least three times using independently generated virus preparations. On days 0, 2, 4, 6, and 8 of infection, 100-μl aliquots of culture supernatants were filtered and stocked for measurements of p24 antigen concentration and replaced with equal amount of fresh medium with or without NVP. The concentrations of p24 in the supernatants were determined by chemiluminescence enzyme immunoassay (CLEIA) kit (Fuji-Rebio, Tokyo, Japan).

Competitive HIV-1 replication assay

Freshly prepared H9 cells (3×10^5) were exposed to virus preparations (300 BFU) to be examined for their replication ability and cultured in the presence or absence of NVP as described previously (Gatanaga et al., 2002; Kosalaraksa et al., 1999; Yoshimura et al., 1999). On day 1 in culture, one-third of the infected H9 cells were harvested and washed twice with PBS, and cellular DNA was extracted with Smi-test nucleic acid extraction kit. Purified DNAs were subjected to nested PCR for sequencing HIV-1 RT gene. Every 7 days, the supernatant of the virus culture was transmitted to new uninfected H9 cells, the cells harvested at each passage were subjected to direct DNA sequencing of HIV-1 RT gene, and the viral population change was determined by the relative peak height on sequencing electrogram. The persistence of the original amino acid substitution was confirmed for all infectious clones used in this assay.

Structural analysis of mutations in HIV-1 RT

To examine the interaction of HIV-1 RT with NVP, the SYBYL 6.7 (http://www.tripos.com/, Tripos Associates, St. Louis, MO) on a Silicon Graphics Octane2 workstation was employed. The site of the enzyme ligand complex was constructed based on the previously reported X-ray structure of the covalently trapped catalytic complex of HIV-1 RT with NVP (Protein Data Bank entry 1FKP) (Ren et al., 2000).

Acknowledgments

The authors thank Yukiko Takahashi and Fujie Negishi for sample preparation. This study was supported in part by the Grant-in-Aid for AIDS research from the Ministry of Health, Labor, and Welfare of Japan (H15-AIDS-001) and by the Organization of Pharmaceutical Safety and Research (01-4).

References

Briones, C., Perez-Olmeda, M., Rodriguez, C., del Romero, J., Hertogs, K., Soriano, V., 2001. Primary genotypic and phenotypic HIV-1 drug resistance in recent seroconverters in Madrid. J. Acquired Immune Defic. Syndr. 26, 145–150.

Cohen, J., 2003. Thailand's do-it-yourself therapy. Science 301, 1662.

Demeter, L.M., Meehan, P.M., Morse, G., Fischl, M.A., Para, M., Powderly, W., Leedom, J., Holden-Wiltse, J., Greisberger, C., Wood, K., Timpone Jr., J., Wathen, L.K., Nevin, T., Resnick, L., Batts, D.H., Reichman, R.C., 1998. Phase I study of atevirdine mesylaye (U-87201E) monotherapy in HIV-1-infected patients. J. Acquired Immune Defic. Syndr. 19, 135–144.

Demeter, L.M., Shafer, R.W., Meehan, P.M., Holden-Wiltse, J., Fischl, M.A., Freimuth, W.W., Para, M.F., Reichman, R.C., 2000. Delavirdine susceptibilities and associated reverse transcriptase mutations in human immunodeficiency virus type 1 isolates from patients in a phase I/II trial of delavirdine monotherapy (ACTG 260). Antimicrob. Agents Chemother. 44, 794–797.

Devereux, H.L., Youle, M., Johnson, M.A., Loveday, C., 1999. Rapid decline in detectability of HIV-1 drug resistance mutations after stopping therapy. AIDS 13, F123–F127.

Duwe, S., Brunn, M., Altmann, D., Hamouda, O., Schmidt, B., Walter, H., Pauli, G., Kucherer, C., 2001. Frequency of genotypic and phenotypic drug-resistant HIV-1 among therapy-naïve patients of German Seroconverter Study. J. Acquired Immune Defic. Syndr. 26, 266–273.

Gatanaga, H., Oka, S., Ida, S., Wakabayashi, T., Shioda, T., Iwamoto, A., 1999. Active HIV-1 redistribution and replication in the brain with HIV encephalitis. Arch. Virol. 144, 29–43.

Gatanaga, H., Suzuki, Y., Tsang, H., Yoshimura, K., Kavlick, M.F., Nagashima, K., Gorelick, R.J., Mardy, S., Tang, C., Summers, M.F., Mitsuya, H., 2002. Amino acid substitutions in Gag protein at non-cleavage sites are indispensable for the development of a high multitude of HIV-1 resistance against protease inhibitors. J. Biol. Chem. 277, 5952–5961.

Grant, R.M., Hecht, F.M., Warmerdam, M., Liu, L., Liegler, T., Petropoulos, C.J., Hellmann, N.S., Chesney, M., Busch, M.P., Kahn, J.O., 2002. Time trends in primary HIV-1 drug resistance among recently infected persons. JAMA 288, 181–188.

Guay, L.A., Musoke, P., Fleming, T., Bagenda, D., Allen, M., Nakabiito, C., Sherman, J., Bakaki, P., Cucar, C., Deseyve, M., Emel, L., Mirochnick, M., Fowler, M.G., Mofenson, L., Miotti, P., Dransfield, K., Bray, D., Mmiro, F., Jackson, J.B., 1999. Intrapartum and neonatal single-dose nevirapine compared with zidovudine for prevention of mother-to-child transmission of HIV-1 in Kampala, Uganda: HIVNET 012 randomized trial. Lancet 354, 795–802.

Hachiya, A., Aizawa-Matsuoka, S., Tanaka, M., Takahashi, Y., Ida, S., Gatanaga, H., Hirabayashi, Y., Kojima, A., Tatsumi, M., Oka, S., 2001. Rapid and simple phenotypic assay for drug susceptibility of human immunodeficiency virus type 1 by using CCR5-expressing HeLa/CD4$^+$ cell clone 1-10 (MAGIC-5). Antimicrob. Agents Chemother. 45, 495–501.

Hachiya, A., Matsuoka-Aizawa, S., Tsuchiya, K., Gatanaga, H., Kimura, S., Tatsumi, M., Oka, S., 2003. "All-in-One Assay", a direct phenotypic anti-human immunodeficiency virus type 1 drug resistance assay for three-drug combination therapies that takes into consideration in vivo drug concentrations. J. Virol. Methods 111, 43–53.

Hirsch, M.S., Brun-Vezinet, F., Clotet, B., Conway, B., Kuritzkes, D.R., D'Aquila, R.T., Demeter, L.M., Hammer, S.M., Johnson, V.A., Loveday, C., Mellors, J.W., Jacobsen, D.M., Richman, D.D., 2003. Antiretroviral drug resistance testing in adults infected with human immunodeficiency virus type 1: 2003 Recommendations of an international AIDS society-USA panel. Clin. Infect. Dis. 37, 113–128.

Huang, H., Chopra, R., Verdine, G.L., Harrison, S.C., 1998. Structure of a covalently trapped catalytic complex of HIV-1 reverse transcriptase: implications for drug resistance. Science 282 (5394), 1669–1675.

Ida, S., Gatanaga, H., Shioda, T., Nagai, Y., Kobayashi, N., Shimada, K., Iwamoto, A., Oka, S., 1997. HIV type 1 V3 variation dynamics in vivo: long-term persistence of non-syncytium-inducing genotypes and transient presence of syncytium-inducing genotypes during the course of progressive AIDS. AIDS Res. Hum. Retroviruses 13, 1597–1609.

Johnson, V.A., Brun-Vezinet, F., Clotet, B., Conway, B., D'Aquila, R.T., Demeter, L.M., Kuritzkes, D.R., Pillay, D., Schapiro, J.M., Telenti, A., Richman, D.D., International AIDS Society-USA Drug Resistance Mutations Group, 2003. Drug resistance mutations in HIV-1. Top. HIV Med. 11, 215–221.

Kodama, E.I., Kohgo, S., Kitano, K., Machida, H., Gatanaga, H., Shigeta, S., Matsuoka, M., Ohrui, H., Mitsuya, H., 2001. 4'ethynyl nucleoside analogs: potent inhibitors of multidrug-resistant human immunodeficiency virus variants in vitro. Antimicrob. Agents Chemother. 45, 1539–1546.

Kosalaraksa, P., Kavlick, M.F., Maroun, V., Le, R., Mitsuya, H., 1999. Comparative fitness of multi-dideoxynucleoside-resistant human immunodeficiency virus type 1 (HIV-1) in an in vitro competitive HIV-1 replication assay. J. Virol. 73, 5356–5363.

Little, S.J., Holte, S., Routy, J.P., Daar, E.S., Markowitz, M., Collier, A.C., Koup, R.A., Mellors, J.W., Connick, E., Conway, B., Kilby, M., Wang, L., Whitcomb, J.M., Hellmann, N.S., Richmann, D.D., 2002. Antiretroviral-drug resistance among patients recently infected with HIV. N. Engl. J. Med. 347, 385–394.

Marseille, E., Kahn, J.G., Mmiro, F., Guay, L., Musoke, P., Fowler, M.G., Jackson, J.B., 1999. Cost effectiveness of single-dose nevirapine regimen for mothers and babies to decrease vertical HIV-1 transmission in sub-Saharan Africa. Lancet 354, 803–809.

Miller, V., Sabin, C., Hertogs, K., Bloor, S., Martinez-Picado, J., D'Aquila, R., Larder, B., Lutz, T., Gute, P., Weidmann, E., Rabenau, H., Phillips, A., Staszewski, S., 2000. Virological and immunological effects of treatment interruptions in HIV-1 infected patients with treatment failure. AIDS 14, 2857–2867.

Morris, L., Pillay, C., Chezzi, C., Lupondwana, P., Ntsala, M., Levin, L., Venter, F., Martinson, N., Gray, G., McIntyre, J., 2003. Low frequency of the V106M mutation among HIV-1 subtype C-infected pregnant women exposed to nevirapine. AIDS 17, 1698–1700.

Parkin, N.T., Deeks, S.G., Wrin, M.T., Yap, J., Grant, R.M., Lee, K.H., Heeren, D., Hellmann, N.S., Petropoulos, C.J., 2000. Loss of antiretroviral drug susceptibility at low viral load during early virological failure in treatment-experienced patients. AIDS 14, 2877–2887.

Penzak, S.R., Acosta, E.P., Turner, M., Tavel, J.A., Masur, H., 2003. Analysis of generic nevirapine products in developing countries. JAMA 289, 2648–2649.

Ren, J., Milton, J., Weaver, K.L., Short, S.A., Stuart, D.I., Stammers, D.K., 2000. Structural basis for the resilience of efavirenz (DMP-266) to drug resistance mutations in HIV-1 reverse transcriptase. Structure Fold Des. 8, 1089–1094.

Salomon, H., Wainberg, M.A., Brenner, B., Quan, Y., Rouleau, D., Cote, P., LeBlanc, R., Lefebvre, E., Spira, B., Tsoukas, C., Sekaly, R.P., Conway, B., Mayers, D., Routy, J.P., 2000. Prevalence of HIV-1 resistant to antiretroviral drugs in 81 individuals newly infected by sexual contact or injecting drug use. Investigators of the Quebec primary infection study. AIDS 14, F17–F23.

Sarafianos, S.G., Das, K., Ding, J., Boyer, P.L., Hughes, S.H., Arnold, E., 1999. Touching the heart of HIV-1 drug resistance: the fingers close down on the dNTP at the polymerase active site. Chem. Biol. 6, R137–R146.

Simon, V., Vanderhoeven, J., Hurley, A., Ramratnam, B., Louie, M., Dawson, K., Parkin, N., Boden, D., Markowitz, M., 2002. Evolving patterns of HIV-1 resistance to antiretroviral agents in newly infected individuals. AIDS 16, 1511–1519.

Sullivan, J.L., 2003. Prevention of mother-to-child transmission of HIV—What next? J. Acquired Immune Defic. Syndr. 34, S67–S72.

Verhofstede, C., Wanzeele, F.V., Van Der Gucht, B., De Cabooter, N., Plum, J., 1999. Interruption of reverse transcriptase inhibitors or a switch from reverse transcriptase to protease inhibitors resulted in a fast reappearance of virus strains with a reverse transcriptase inhibitor-sensitive genotype. AIDS 13, 2541–2546.

Yoshimura, K., Feldman, R., Kodama, E., Kavlick, M.F., Qiu, Y.L., Zemlicka, J., Mitsuya, H., 1999. In vitro induction of human immunodeficiency virus type 1 variants resistant to phosphoralaninate prodrugs of *c*-methylenecyclopropane nucleoside analogues. Antimicrob. Agents Chemother. 43, 2479–2483.

Modified Dynabeads Method for Enumerating CD4+ T-Lymphocyte Count for Widespread Use in Resource-Limited Situations

Xiuqiong Bi,† Hiroyuki Gatanaga,* Mari Tanaka,* Miwako Honda,* Setsuko Ida,* Satoshi Kimura,* and Shinichi Oka**

Summary: The Dynabeads method showed the potential for enumerating CD4+ T lymphocytes (CD4 count) in HIV-1–infected individuals. The large volume of Dynabeads required for 1 sample and complex procedure made the method expensive and not easy for use, however. To decrease the cost and simplify the procedure, we reduced the volume of the Dynabeads, added wash times, and skipped over the staining step so as to count the CD4 cells directly under an optical microscope. The CD4 count of 246 blood samples using our modified Dynabeads method (DynabeadsCD4) showed a significant correlation with that obtained by flow cytometry (FlowcytoCD4) (r = 0.91 [$P < 0.0001$]; slope = 1.03, intercept = −16). The sensitivity and specificity for a CD4 count less than 200 cells/μL were 79% and 94%, and for a CD4 count less than 350 cells/μL, the sensitivity and specificity were 95% and 88%, respectively. The positive and negative predictive values for a CD4 count less than 350 cells/μL were 97% and 83%, respectively. The systematic error was 8 cells/μL (95% confidence interval [CI]: 0.4–16). The cost of Dynabeads for 1 sample was less than $1.00; thus, the estimated cost per DynabeadsCD4 test is less than $3.00, including the cost of other disposable materials. Our modified method is simple, economic, and accurate enough to monitor antiretroviral therapy in resource-limited situations.

Key Words: CD4, monitoring, Dynabeads, resource-limited situations

(*J Acquir Immune Defic Syndr* 2005;38:1–4)

The CD4+ T-lymphocyte count (CD4 count) is an important surrogate marker for the clinical course of HIV infection, such as initiation of prophylactic treatment of opportunistic infections, initiation of antiretroviral therapy (ART), and monitoring the response to ART.[1–4] In developed countries, the CD4 count is usually measured by flow cytometry, which is considered to be the standard reference method.[3,4] In resource-limited areas, however, flow cytometry is available only in limited settings such as tertiary medical centers because it requires expensive reagents and well-trained technicians. Furthermore, equipment maintenance is another difficult issue, because a technical support system is needed in areas afflicted with frequent electrical power failures, which could potentially cause machine-related problems.

In recent years, lower cost and less technically demanding methods for enumerating CD4 cells have been tried but have not been used widely even in resource-limited settings for various reasons.[4,5] In the World Health Organization (WHO) guidelines for treatment of HIV-infected individuals in resource-limited environments, a total lymphocyte count (TLC) of 1200 cells/μL is recommended to represent a CD4 count threshold of 200 cells/μL in making a decision regarding therapy when the CD4 count is unavailable.[1] In addition, various research groups have recommended the use of a TLC,[5] absolute lymphocyte count or TLC,[6] and TLC combined with hemoglobin measurement[7] as surrogate markers for monitoring ART. These studies suggested that the lymphocyte count might have some value in monitoring ART. The lymphocyte count is readily available and inexpensive, but it is not sufficiently adequate to predict the absolute CD4 count in many settings.[4]

Among several low-cost and less technically demanding methods,[8–15] the Dynabeads assay, which uses magnetic particles coated with a monoclonal antibody to CD4 to capture CD4+ cells, seems to be a good candidate as an alternative to flow cytometry based on its good correlation with the results of flow cytometry.[8,10,11,13] According to the protocol recommended by the manufacturer, however, CD4 and CD8 cells are enumerated at the same time using a large volume of Dynabeads. The large volume of Dynabeads used in each assay is also relatively expensive (approximately $5), particularly for poor settings. In addition, division of the samples into 2 aliquots during the procedure might jeopardize the accuracy of the results. Moreover, in this assay, the cells are lysed and nuclei are stained to count them, which makes the operation complex.

For monitoring ART in HIV infections, only the CD4 component is necessary and only the CD4 count (not CD8 count) is mentioned in ART guidelines.[1,2] For this reason,

Received for publication May 31, 2004; accepted September 14, 2004.

From the *AIDS Clinical Center, International Medical Center of Japan, Tokyo, Japan; and †Graduate School of Medicine, University of Tokyo, Tokyo, Japan.

Supported in part by a grant-in-aid for AIDS Research from the Ministry of Health, Labor, and Welfare of Japan (H15-AIDS-001, H15-International Medical Cooperative Study-03), by the Organization of Pharmaceutical Safety and Research (01-4), and by the Japanese Foundation for AIDS Prevention (X.B.).

Reprints: Shinichi Oka, AIDS Clinical Center, International Medical Center of Japan, 1-21-1 Toyama, Shinjuku-ku, Tokyo 162-8655, Japan (e-mail: oka@imcj.hosp.go.jp).

further modifications are needed for the expanded use of the CD4 count in resource-limited areas. In the present study, we modified the protocol to make it simple and inexpensive so that it could be applied widely in resource-limited facilities.

MATERIALS AND METHODS

Study Population and CD4 Enumeration

This study included 242 adult patients infected with HIV-1 who regularly consulted the AIDS Clinical Center of the International Medical Center of Japan between June and October 2003. The inclusion criteria were a CD4 count less than 1000 cells/μL and consent granted to participate in the study. Patient age ranged from 20 to 78 years (mean ± SD: 40 ± 11.5). A total of 315 blood samples were collected using EDTA-containing tubes and tested for CD4 count within 4 hours by flow cytometry (FlowcytoCD4; Coulter-EPICS XL-MCL, Beckman-Coulter, Fullerton, CA) with CD45–fluorescein isothiocyanate (FITC)/CD4-phycoerythrin (RD1)/CD8-pheycoerythrin-Texas Red (ECD)/CD3-pheycoerythrin-cyanin 5.1 (PC5) (Beckman-Coulter). The CD4 cell count in the rest of the blood sample was enumerated using Dynabeads (Dynabeads CD4; Dynal Biotech ASA, Oslo, Norway) within 24 hours. When different protocols such as 25-μL and 5-μL volumes of CD4 Dynabeads or 10 and 30 minutes of incubation time were compared, the same sample was used in each experiment.

Modified Protocol (Original Protocol) of the Dynabeads Method

A well-mixed whole-blood sample (125 μL) was placed into a 1.5-mL microtube containing 375 μL (350 μL) of buffer (0.1% bovine serum albumin in phosphate-buffered saline [PBS]). CD14 Dynabeads were suspended with buffer (1:1 diluted buffer); 5 μL (25 μL) of CD14 Dynabeads was then added to the microtube containing the blood sample and the tube was inverted several times and then incubated in Dynal MX-1 for 10 minutes. The tube was spun down in a microcentrifuge and then placed in magnetic particle concentration for microcentrifuge tubes (Dynal MPC-S) (6 tubes per batch) for 2 minutes, followed by transfer of the entire volume (division into 2 200-μL aliquots) of monocyte-depleted blood into a new microtube. In the next step, 5 μL (25 μL) of CD4 Dynabeads was added to the tube and incubated in Dynal MX-1 for 30 minutes (10 minutes). The cells were washed with 500 μL of buffer, vortexed gently, and spun down; the tube was then placed in Dynal MPC-S for 2 minutes, the wash buffer was discarded, and the tube was removed from the Dynal MPC-S. The cells were washed 3 more times (once), resuspended by adding 125 μL of buffer, and kept at 4°C until counting (50 μL of lysing solution was added, followed by thorough vortexing for resuspension, and the cells were allowed to stand for 5 minutes, after which 50 μL of acridine orange staining solution was added and the sample was kept in darkness until counting). Finally, the sample was vortexed well, 10 μL of cells was applied to a hemocytometer, and the mononuclear cells with attached Dynabeads were counted as $CD4^+$ cells under a light microscope (the number of nuclei was determined under a fluorescence microscope). After reducing the volume of CD4 Dynabeads, it was not difficult to count the CD4 cells under an optical microscope, even without staining. All procedures were performed at room temperature at approximately 23°C. All Dynabeads-related equipments and reagents were products of Dynal Biotech ASA.

Statistical Analysis

All data are expressed as mean ± SD. StatView v5.0 software was used to analyze the correlation and single linear regression between DynabeadsCD4 and FlowcytoCD4. *P* values were calculated by 2-sided test and considered as significant if at a level less than 5%. All confidence intervals were 2-sided, with a significant level of 5%.

RESULTS

First, we examined the influence of a reduced volume of CD14 (from 12.5 μL to 5 μL) Dynabeads on monocyte depletion. The percentage of monocytes in 5 blood samples was analyzed by flow cytometry before and after treatment with 5 μL of CD14 Dynabeads. The result showed that 5 μL of CD14 Dynabeads deleted 92.4% to 97.5% (average = 95.6%) of monocytes from 125 μL of whole blood. The remaining experiments were performed using 5 μL of CD14 Dynabeads. Next, we examined the influence of a reduced volume of CD4 Dynabeads on the CD4 count in 23 samples. The volume of CD4 Dynabeads was reduced from 25 μL to 5 μL, but the incubation time was still 10 minutes (like that of original protocol), which we called modified protocol 1. CD4 counts by the original protocol and modified protocol 1 correlated significantly with those determined by flow cytometry: DynabeadsCD4 by the original protocol ($r = 0.90$ [$P < 0.0001$]; slope = 1.05, intercept = −32) and DynabeadsCD4 by modified protocol 1 ($r = 0.92$ [$P < 0.0001$]; slope = 1.05, intercept = 26). These results indicated that DynabeadsCD4 obtained by using the reduced volume of CD4 Dynabeads with a 10-minute CD4 separation correlated well with FlowcytoCD4. When the number of samples was increased to 56, however, the mean DynabeadsCD4 of 56 samples by modified protocol 1 was 269 ± 140 cells/μL compared with a mean FlowcytoCD4 of 336 ± 178 cells/μL (Table 1). The difference was −67 cells/μL ($P < 0.0001$). This result suggested that the 10-minute CD4 separation time was too short. We then examined the effect using a reduced volume of Dynabeads and a different incubation time.

Next, with 5 μL of CD4 Dynabeads, we lengthened the CD4 separation time from 10 minutes to 30 minutes in 34 samples. The correlations between DynabeadsCD4 and FlowcytoCD4 were $r = 0.91$ ($P < 0.0001$) and $r = 0.94$ ($P < 0.0001$), with slopes of 1.05 and 1.0 and intercepts of 22 and 8, for 10 and 30 minutes of incubation time, respectively. The mean difference with flowcytoCD4 was −32 cells/μL ($P = 0.008$) and −8 cells/μL ($P = 0.42$), respectively. According to these data, the 30-minute incubation time for CD4 separation yielded a better result than that of the 10-minute incubation time. We then fixed the protocol as 5 μL of CD14 Dynabeads with 10 minutes of incubation time and 5 μL of CD4

TABLE 1. DynabeadsCD4 Determined by Different Protocols Compared with FlowcytoCD4

Protocol	Mean ± SD (Cells/μL)		Mean Difference		Regression Line		
	DynabeadsCD4	FlowcytoCD4	Cells/μL (95% CI)	*P*	Intercept	Slope	r^2
Original (n = 59)	364 ± 166	372 ± 193	−8 (−32 to 16)	0.521	−2	1.026	0.775
Modified 1 (n = 56)*	269 ± 140	336 ± 178	−67 (−93 to −41)	<0.0001	50	1.061	0.698
Modified 2 (n = 246)†	262 ± 136	254 ± 154	8 (0.4 to 16)	0.0396	−16	1.031	0.829

†Modified 2 (the final one): modified protocol with 30 minutes of CD4 separation.
*Modified 1: modified protocol with 10 minutes of CD4 separation.
$P > 0.05$ for all intercepts, $P < 0.0001$ for all slopes and r^2.

Dynabeads with 30 minutes incubation time (which we called modified protocol 2) and tested 246 samples. DynabeadsCD4 showed a significant correlation with FlowcytoCD4 ($r = 0.91$ [$P < 0.0001$]; slope = 1.03, intercept = −16; Fig. 1). At less than 200 cells/μL, the sensitivity and specificity of DynabeadsCD4 compared with FlowcytoCD4 were 79% and 94%, respectively, and at less than 350 cells/μL, the sensitivity and specificity were 95% and 88%, respectively. The mean DynabeadsCD4 was 262 ± 135 cells/μL and that of FlowcytoCD4 was 254 ± 154 cells/μL (see Table 1). The difference in the mean values was 8 cells/μL (95% confidence interval [CI]: 0.4–16; $P = 0.04$), with a random error of 64 cells/μL. The positive and negative predictive values of DynabeadsCD4 and FlowcytoCD4 for less than 200 cells/μL and less than 350 cells/μL were 90% and 87% and 97% and 83%, respectively. Other factors (eg, on therapy vs. off therapy, male vs. female) had no influence on DynabeadsCD4 (data not shown).

Table 2 shows the results of a comparison between the original protocol and our modified protocol. In our modified protocol, volumes of CD14 and CD4 Dynabeads were reduced from 12.5 μL and 25 μL, respectively, to 5 μL each against 125 μL of whole blood. Accordingly, the cost of the Dynabeads test decreased from $2.84 to $0.89. The incubation time for CD4 separation was prolonged to 30 minutes to obtain a better yield. In our protocol, after monocyte depletion, we transferred all treated blood to a new microtube for CD4 cell separation because we did not consider the CD8 count. We also skipped over lysis and nuclear staining steps so as to simplify the procedure.

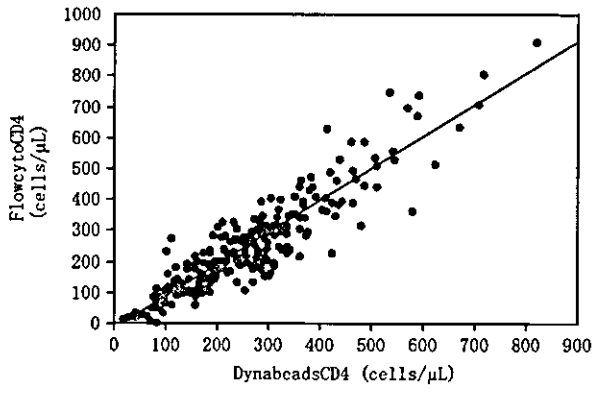

FlowcytoCD4 = -16.484 + 1.031 × DynabeadsCD4; $r^2 = 0.829$

FIGURE 1. Correlation analysis of CD4+ T-lymphocyte count (CD4 count) using Dynabeads method and CD4 count using flow cytometry.

DISCUSSION

To attain the "3 by 5" goal of effective ART promoted by the WHO, precise monitoring of ART is indispensable. Low cost, in addition to good accuracy, is thus an important issue. In this regard, maintenance of a "high-tech" machine for long-term monitoring may be impossible. The Dynabeads method is currently used as an alternative method to flow cytometry for CD4 count in a number of countries. In this study, we successfully modified the protocol of the Dynabeads method to make it more suitable in resource-limited areas with 2 goals in mind: reasonable cost and sufficient accuracy.

TABLE 2. Comparison Between the Original Protocol and Modified Protocol 2 for Enumeration of CD4 Count

Step	Original Protocol	Modified Protocol 2
Buffer (μL)	350	375
Blood (μL)	125	125
CD14 Dynabeads (μL)	25 (1:1 dilution)	5
Incubation temperature (°C)	RT	RT
Incubation duration (min)	10	10
Monocyte-depleted supernatant (μL)	200*	505†
CD4 Dynabeads (μL)	25	5
Incubation temperature (°C)	RT	RT
Incubation duration (min)	10	30
Repeat of washing (total min)	2 (10 min)	4 (20 min)
Staining time (min)	5 min	—
Resuspension volume (μL)	—	125
Time of total experiment per sample (min)	50	75
Samples comfortably analyzed per operator	12–18	12–18
Cost of CD14 Dynabeads ($)	1.63	0.65
Cost of CD4 Dynabeads ($)	1.21	0.24
Total cost of Dynabeads ($)	2.84	0.89

*Transferring 200 μL to a new tube.
†Transferring the entire volume to a new tube.
Values are for 1 test.
RT indicates room temperature (approximately 23°C).

In the present study, DynabeadsCD4 obtained by using the original protocol also showed a good result (see Table 1). During the operation, we found 2 problems with the original protocol, however. One was the transfer of 200 μL of blood from 500 μL of blood to a new tube after monocyte depletion. This step might lead to inaccurate results because we could not mix the blood well while the tube was on the Dynal MPC-S. The other was that too many free Dynabeads (which did not attach to CD4 cells) and red blood cells were identified when the cells were counted under a light microscope. This might be the reason for recommending lysis of the cells, staining the nuclei, and using a fluorescent microscope in the last step of the original protocol. In our modified protocol, the entire sample was transferred to a new tube after monocyte depletion. The number of free Dynabeads decreased after the volume of CD4 Dynabeads was reduced. Furthermore, we washed the sample 4 times after CD4 cell separation in spite of the original protocol recommending washing only twice. The red blood cells could be almost completely removed by 4 washes, especially when the washing buffer had been discarded completely at each wash. These modifications made a direct count under a light microscope possible.

After reduction of the volume of Dynabeads used in the assay, the cost of reagents used for analysis of 1 sample decreased to less than $1.00. Thus, the total cost of 1 CD4 count, including other disposable materials such as syringes, tubes, and tips, could be less than $3.00.

In conclusion, the present study demonstrated that our final modified protocol of Dynabeads assay could be used as a good alternative to flow cytometry with sufficient accuracy, reliability, and simplicity at a reasonable cost. Therefore, the assay could be suitable for monitoring ART in resource-limited settings.

ACKNOWLEDGMENTS

The authors thank Naomi Wakasugi (International Medical Center of Japan) and Kenji Tamura (WHO) for their helpful suggestions and encouragement during the study.

REFERENCES

1. World Health Organization. Scaling up antiretroviral therapy in resource limited settings: guidelines for a public health approach. Available at: http://www.who.int/hiv/. Accessed April 2002.
2. Department of Health and Human Services. Guidelines for the use of antiretroviral agents in HIV-1-infected adults and adolescents. Available at: http://AIDsinfo.nih.gov. Accessed July 14, 2003.
3. Brando B, Barnett D, Janossy G, et al. Cytofluorimetric methods for assessing absolute numbers of cell subsets in blood. *Cytometry.* 2000; 42:327–346.
4. Crowe S, Turnbull S, Oelrichs R, et al. Monitoring of human immunodeficiency virus infection in resource-constrained countries. *Clin Infect Dis.* 2003;37(Suppl 1):S25–S35.
5. Badri M, Wood R. Usefulness of total lymphocyte count in monitoring highly active antiretroviral therapy in resource-limited settings. *AIDS.* 2003;17:541–545.
6. Jacobson AM, Liu L, Khayam-Bashi H, et al. Absolute or total lymphocyte count as a marker for the CD4 T lymphocyte criterion for initiating antiretroviral therapy. *AIDS.* 2003;17:917–919.
7. Spacek AL, Griswold M, Quinn CT, et al. Total lymphocyte count and hemoglobin combined in an algorithm to initiate the use of highly active antiretroviral therapy in resource-limited settings. *AIDS.* 2003;17:1311–1317.
8. Diagbouga S, Chazallon C, Kazatchkine MD, et al. Successful implementation of a low-cost method for enumerating CD4+ T lymphocytes in resource-limited settings: the ANRS 12-26 study. *AIDS.* 2003;17:2201–2208.
9. Brinchmann JE, Leivestad T, Vartdal F. Quantification of lymphocyte subsets based on cells directly from blood. *J Immunogenet.* 1989;16:177–183.
10. Didier J, Kazatchkine M, Demouchy C, et al. Comparative assessment of five alternative methods for CD4 T-lymphocyte enumeration for implementation in developing countries. *J Acquir Immune Defic Syndr.* 2001; 26:193–195.
11. Lyamuya EF, Kagoma C, Mbena EC, et al. Evaluation of the FACScount, TRAx CD4 and Dynabeads methods for CD4 lymphocyte determination. *J Immunol Methods.* 1996;195:103–112.
12. Nicholson JK, Velleca W, Jubert S, et al. Evaluation of alternative CD4 technologies for the enumeration of CD4 lymphocyte. *J Immunol Methods.* 1994;177:43–54.
13. Lyamuya EF, Schechter M, Echeverria de Perez G, et al. Multicentre evaluation of alternative methods for CD4 lymphocyte determination [abstract Mo.A.513]. Presented at the International AIDS Conference, Vancouver, July 1996.
14. Carella AV, Moss MW, Provost V, et al. A manual bead assay for the determination of absolute CD4+ and CD8+ lymphocyte counts in human immunodeficiency virus-infected individuals. *Clin Diagn Lab Immunol.* 1995;2:623–625.
15. Gaudernack G, Lundin KE. Rapid immunomagnetic phenotyping of cells. *J Immunogenet.* 1989;16:169–175.

別紙5

研究成果の刊行に関する一覧表

発表者氏名	論文タイトル名	発表誌名	巻号	ページ	出版年
Yokomaku Y, Miura H, Tomiyama H, Kawana-Tachikawa A, **Takiguchi M,** Kojima A, Nagai Y, Iwamoto A, Matsuda Z, and Ariyoshi K.	Impaired Processing and Presentation of Cytotoxic T-Lymphocyte (CTL) Epitope is a Major Escape Mechanism from CTL Immune Pressure in Human Immunodeficiency Virus Type 1 Infection.	***J Virol***	78	1324-1332	2004
Tomiyama H, Takata H, Matsuda T, and **Takiguchi M.**	Phenotypic classification of human CD8+ T cells reflecting their function: An inverse correlation between quantitative expression of CD27 and cytotoxic effector function.	***Eur J Immunol***	34	999-1010	2004
Takata H, Tomiyama H, Fujiwara M, Kobayashi N, and **Takiguchi M.**	Expression of Chemokine Receptor CXCR1 on Human Effector CD8+ T Cells.	***J Immunol (Cutting Edge)***	173	2231-2235	2004
Ueno T, Tomiyama H, Fukjiwara M, **Oka S,** and **Takiguchi M.**	Functionally impaired HIV-specific CD8 T cells show high-affinity TCR-ligand interactions.	***J Immunol***	173	5451-5457	2004
Ueno T, Fujiwara M, Tomiyama H, Onodera M, and **Takiguchi M.**	Reconstitution of anti-HIV effector functions of primary human CD8 T lymphocytes by transfer of HIV-specific αβ TCR genes.	***Eur J Imunol***	34	3379-3388	2004
Kobayashi N, Takata H, Yokota S, and **Takiguchi M.**	Down-regulation of CXCR4 expression on human CD8+ T cells during peripheral differentiation.	***Eur J Immunol***	34	3370-3378	2004
Tomiyama H, Fujiwara M, **Oka S,** and **Takiguchi M.**	Epitope-dependent effect of Nef-mediated HLA class I down-regulation on ability of HIV-1-specific CTL to suppress HIV-1 replication.	***J Immunol (Cutting Edge)***	174	36-40	2004

発表者氏名	論文タイトル名	発表誌名	巻号	ページ	出版年
Satoh M, Takamiya Y, **Oka S**, Tokunaga K, and **Takiguchi M.**	*: Identification and characterization of HIV-1-specific CD8+ T cell epitopes presented by HLA-A*2601.	***Vaccine*** (in the press)			

JOURNAL OF VIROLOGY, Feb. 2004, p. 1324–1332
0022-538X/04/$08.00+0 DOI: 10.1128/JVI.78.3.1324–1332.2004

Vol. 78, No. 3

Impaired Processing and Presentation of Cytotoxic-T-Lymphocyte (CTL) Epitopes Are Major Escape Mechanisms from CTL Immune Pressure in Human Immunodeficiency Virus Type 1 Infection

Yoshiyuki Yokomaku,[1] Hideka Miura,[1] Hiroko Tomiyama,[2] Ai Kawana-Tachikawa,[3] Masafumi Takiguchi,[2] Asato Kojima,[4] Yoshiyuki Nagai,[1]† Aikichi Iwamoto,[3] Zene Matsuda,[1] and Koya Ariyoshi[1]*

AIDS Research Center[1] and Department of Pathology,[4] National Institute of Infectious Diseases, and Department of Infectious Diseases, Institute of Medical Science, University of Tokyo,[3] Tokyo, and Center for AIDS Research, Kumamoto University, Kumamoto,[2] Japan

Received 21 April 2003/Accepted 7 October 2003

Investigating escape mechanisms of human immunodeficiency virus type 1 (HIV-1) from cytotoxic T lymphocytes (CTLs) is essential for understanding the pathogenesis of HIV-1 infection and developing effective vaccines. To study the processing and presentation of known CTL epitopes, we prepared Epstein-Barr virus-transformed B cells that endogenously express the *gag* gene of six field isolates by adopting an *env/nef*-deletion HIV-1 vector pseudotyped with vesicular stomatitis virus G protein and then tested them for the recognition by Gag epitope-specific CTL lines or clones. We observed that two field variants, SLENTVAVL and SVYNTV ATL, of an A*0201-restricted Gag CTL epitope SLYNTVATL, and three field variants, KYRLKHLVW, QYRLKHIVW, and RYRLKHLVW, of an A24-restricted Gag CTL epitope KYKLKHIVW escaped from being killed by the CTL lines, despite the fact that they were recognized when the synthetic peptides corresponding to these variant sequences were exogenously loaded onto the target cells. Thus, their escape is likely due to the changes that occur during the processing and presentation of epitopes in the infected cells. Mutations responsible for this mode of escape were located within the epitope regions rather than the flanking regions, and such mutations did not influence the virus replication. The results suggest that the impaired antigen processing and presentation often occur in HIV-1 field isolates and thus are one of the major mechanisms that enable HIV-1 to escape from CTL recognition. We emphasize the importance of testing HIV-1 variants in an endogenous expression system.

Accumulated evidence has indicated a critical role of cytotoxic T lymphocytes (CTLs) in controlling human immunodeficiency virus (HIV) replication during acute and chronic infection (16). Eliciting HIV type 1 (HIV-1)-specific CTLs has been thought to be crucial for effective HIV/AIDS vaccines (15). However, despite the presence of CTLs, the majority of HIV-1-infected cases eventually progress to AIDS, probably as a consequence of the emergence of escape mutants from CTLs (8, 20). Among immunized monkeys, which developed strong cellular immune responses against HIV-1, eventual vaccine failure occurs by viral escape from CTLs (2). Thus, investigating the mechanisms of CTL failure to control the virus is essential to understanding the pathogenesis of HIV-1 infection and to develop HIV/AIDS vaccines.

The high rate of HIV-1 replication in vivo indicates that HIV-1 has tremendous ability to mutate swiftly (9, 30) and to make a dynamic adaptation to host-immune environments (3, 14, 18, 21, 31). Several mutations have been described in CTL epitopes in HIV-1-infected individuals, which result in either a lack of binding to the MHC class I molecule or nonrecognition by T-cell receptor (TCR) (3, 8, 12, 20, 21). Consequently, the virus escapes from CTL recognition. There are other mutations that do not lead to either escape effects (12); very little is known about the influence of these mutations on CTL recognition. CTL antigens are processed and presented on the cell surface in a very complex manner. Peptides are cleaved from endogenously synthesized proteins by proteasome in the cytoplasm and transported into the endoplasmic reticulum by the transporter of antigen presentation. Amino-terminal extended peptides are trimmed to the right size of peptides by aminopeptidases, which exist in both the cytoplasm and the endoplasmic reticulum (23). These steps have various degrees of substrate sequence specificity (17). The generated peptides should have sufficient affinity to bind to a major histocompatibility complex (MHC) class I molecule in the presence of various other peptides derived from host proteins and to maintain the stability of peptide-MHC complexes until they are presented on the cell surface (28). Thus, it is plausible that some amino acid substitutions in the epitope and its flanking regions have a significant influence on antigen processing and presentation. In the present study, we hypothesized that such mutations often enable HIV-1 to escape from CTL recognition.

Conventionally, the intracellular HIV-1 antigen processing and presentation has been studied with recombinant vaccinia viruses expressing an HIV-1 gene (3, 4, 11, 20, 26). Several

* Corresponding author. Mailing address: AIDS Research Center, National Institute of Infectious Diseases, 4-7-1 Gakuen, Musashimurayama, Tokyo, 208-0011 Japan. Phone: 81-42-561-0771. Fax: 81-42-561-7746. E-mail: ariyoshi@nih.go.jp

†Present address: Toyama Institute of Health, Toyama, 939-0363 Japan.

TABLE 1. Characteristics of five HIV-1-infected donors[a]

Donor	HLA type			CD4 count/μl	Virus load (copies/ml)	No. of isolated clones
	A	B	Cw			
IMS1	*0201/2402	52/75	3	286	<400	3
IMS2	*0201/31	27/5101	2	797	<400	2
IMS4	*0207/2402	46/52	1	448	<400	2
IMS6	2402/26	7/5101	7	368	3.6×10^5	3
IMS7	1/−	37/−	6	544	1.3×10^3	3

[a] HLA alleles, CD4 count, viral load, and the number of isolated clones from each donor's sample are shown.

studies have addressed this issue in the context of HIV-infected T cells (4, 29, 32, 33). Most studies, however, have only evaluated a single or a few laboratory-established strains. The CTL recognition of HIV-1 clinical isolates has been evaluated, in most cases, by exogenously applying synthetic variant peptides to the cell surface to replace MHC-bound peptides (8, 12, 20, 21). Very little is known about how the antigenic products of HIV-1 clinical isolates are processed and presented in the infected cells. To address this issue, we prepared CTL target cells that endogenously express the *gag* gene derived from HIV-1 clinical isolates by adopting an *env/nef*-deletion HIV-1-based vector pseudotyped with vesicular stomatitis virus protein G (VSV-G) proteins. Here, we show evidence that HIV-1 escapes from CTL recognition often via the impairment of antigen processing and presentation.

MATERIALS AND METHODS

Subjects. Peripheral blood mononuclear cells (PBMC) were collected from five HIV-1-infected individuals from the HIV clinic affiliated with the Institute of Medical Science, University of Tokyo. Two individuals (IMS1 and IMS2) had no therapy; one individual (IMS6) was off drugs but had received treatment (zidovudine alone) 2 years prior to blood sampling; two individuals (IMS4 and IMS7) had received therapy (zidovudine-lamivudine-indinavir and stavudine-lamivudine-nelfinavir, respectively) but for less than 3 months. CD4 count, viral load, and HLA type of the recruited individuals are shown in Table 1. HLA class 1 typing was initially performed by serology. Subtyping of HLA-A2 was done by a PCR–sequence-specific primer method (Dynal Classic SSP HLA-A2; Dynal A.S., Oslo, Norway).

Isolation and cloning of full-length *gag*. Full-length *gag* was amplified from proviral DNA extracted from the PBMC by nested PCR with *Pfu* DNA polymerase (Strategene, La Jolla, Calif.) and oligonucleotides specific for HIV-1 long terminal repeat (LTR) and reverse transcription (RT) regions. Four oligonucleotides were mixed as outer primers: the sense primers 1U5AS-S (5′-ACTCTG GTADCTAGAGATCCCTCA-3′; the position in HXB2 being 578 to 601) and TAR-2 (5′-TGAGCCTGGGAGCTCTCTGGCT-3′; 478-499) and the antisense primers RT7A-A (5′-TATGTTGAYAGGTGTAGGTC-3′; 2485 to 2504) and RT18A-A (5′-CTACYARTACTGTACCTATAG-3′; 2464 to 2484). Two oligonucleotides were used as inner primers: the sense primer TPBS1-S (5′-AAAA TCTCTAGCAGTGGCGCCCGAACAGG-3′; the position in HXB2 being 622 to 650) and the antisense inner primer PRO6A (5′-ACTGTATCATCTGCTCC TGTRTCTAA-3′; 2322 to 2347). The thermocycling conditions were 95°C for 45 s, 50°C for 45 s, and 72°C for 210 s (30 cycles) and 72°C for 7 min for both primary and secondary PCR. The PCR products were purified by using spin columns (QIAquick PCR purification kit; Qiagen, Santa Clarita, Calif.) and cloned into PT7Blue3 vector by using a commercial cloning kit (Perfectly Blunt cloning kit; Novagen, Dedham, Mass.). Two to three clones for each individual were sequenced by an automated sequencer (ABI Prism 377 automated DNA sequencer; Perkin-Elmer, Norwalk, Conn.) with BigDye terminators (PE Applied Biosystems, Foster City, Calif.). The sequences of *gag* clones that were used in the present study are available under GenBank Accession numbers as follows: AB074049 (IMS1-28), AB074050 (IMS1-29), AB074052 (IMS2-5), AB074058 (IMS4-24), AB074061 (IMS6-34), and AB074064 (IMS7-11).

Construction of HIV-1 vector. The design of HIV-1 vector, pCTLpac, is shown in Fig. 1. The backbone of the vector is derived from an infectious molecular clone, HXB2I:cogpt (22), which lacks the function of *vpr*, *vpu*, and *nef* genes. We deleted a 1.5-kb portion from the *env*-coding region but kept the function of Rev responsive element, Tat, and Rev. The *nef* gene was replaced with the puromycin *N*-acetyltransferase (*pac*) gene (pPUR; BD Biosciences Clontech, Palo Alto, Calif.) by using *Xho*I and *Cla*I sites where the *Cla*I site was introduced by site-directed mutagenesis. *Sbf*I and *Swa*I sites were introduced by site-directed mutagenesis in the upstream of the *gag* (nucleotide 788) and in the *pol* (nucleotide 3717), respectively. The fragment from *Spe*I in the gag (nucleotide 1507) to the *Swa*I was then replaced with that of a previously published vector, pHXB2ev (25), which has a *Not*I site but lacks an *Sbf*I site in the *pol* gene. Consequently, the final construct carries the single *Sbf*I site (nucleotide 788) and the *Not*I site (nucleotide 2275) that corresponds to the 10th codon of protease. These sites were used for incorporating the *gag* clones derived from clinical isolates into the pCTLpac vector. We confirmed that the expected variant sequences were inserted in the vector by sequencing.

Generation of VSV-G pseudotype virus. Subconfluent COS7 cells in 25-cm^2 T flasks (Becton Dickinson, Lincoln Park, N.J.) were cotransfected with 4 μg of pCTLpac and 2 μg of pVSVG (BD Biosciences Clontech), which expresses VSV-G protein, by lipofection (FuGENE6; Roche Molecular Biochemicals, Mannheim, Germany) and then incubated for 48 to 60 h. The supernatant, which contains pseudotype viruses carrying the HIV-1 vector with VSV-G envelope proteins, was harvested, filtered through a 0.45-μm (pore-size) Millex filter (Millipore, Bedford, Mass.), and used as pseudotype virus stocks, some of which were stored at −80°C before use. The amount of p24 antigen in the stocks was measured by p24 antigen capture enzyme-linked immunosorbent assay (ELISA; RETRO-TEK; Zeptometrix Corp., Buffalo, N.Y.). The range of the p24 antigen yield was 40 to 100 ng/ml.

Preparation of target cells by using VSV-G pseudotyped HIV-1 vector. Epstein-Barr virus-transformed B-lymphocyte lines (B-LCLs) were infected with pseudotype virus stocks for 6 h at 37°C. The medium was then replaced with fresh RPMI 1640 (Sigma-Aldrich, St. Louis, Mo.) supplemented with 10% fetal bovine serum (R10; HyClone, Logan, Utah), and the cells were incubated for an additional 36 h. Subsequently, 0.5 μg of puromycin (BD Biosciences Clontech)/ml was added to the R10 medium to select transduced cells. The culture was maintained until the number of transduced cells became sufficient for CTL experiments. When 10^6 B-LCLs were infected with 1 ml of pseudotype virus stocks, the transduction efficiency was 20 to 30%. Usually, more than 10^7 transduced cells were generated within 2 weeks and used as CTL target cells.

To standardize the expression level of Gag protein in target cells, we quantified the amount of extracellular p24 antigen that 10^6 cells per ml of target cells had produced in 24 h. The supernatant was harvested before (supernatant A) and after (supernatant B) the 24 h of culture for the measurement of p24 antigen by p24 antigen capture ELISA (Zeptometrix Corp.). The level of p24 antigen production was defined by the difference in the concentration of p24 antigen between supernatants A and B. If the target cells produced p24 antigen that was >1 ng/ml in 24 h, they were used for CTL experiments, since the specific percent lysis did not significantly differ among target cells producing Gag protein above

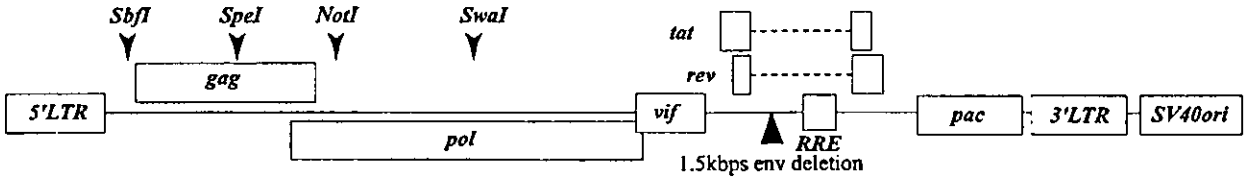

FIG. 1. Structure of pCTLpac. A 1.5-kbp portion of *env* was deleted (▲). Puromycin *N*-acetyltransferase gene (*pac*) was inserted in the *nef* region. The locations of restriction enzyme sites are indicated (▼). RRE, Rev responsive element.

this level (data not shown). We also investigated the level and pattern of protein expression of *gag* variants by Western blot analysis, as previously described (25).

^{51}Cr release experiments with HLA-class I-mismatched target cells in parallel with HLA-class I matched target cells of different donors confirmed that these target cells were recognized by CTLs in an HLA-restricted manner (data not shown). Repeated experiments showed that specific lysis of blank controls was equivalent to that of cells expressing *gag* variants that are known to escape either from TCR recognition or MHC binding. Some examples appear in the Results section below: specific lysis against IMS2-5 (Fig. 3a), IMS4-24 (Fig. 3c), IMS6-34 (Fig. 3e), and HXB2-wild (Fig. 5b). Thus, we regarded the blank control as a negative control.

Preparation of target cells by using recombinant vaccinia viruses. Recombinant vaccinia viruses used in the experiment shown in Fig. 3b were made as previously described (10). HLA-matched B-LCLs were infected with recombinant vaccinia viruses at a multiplicity of infection of 3:1 overnight before being tested in a ^{51}Cr release assay.

Effector cells. Peptide-specific CTL lines were induced from PBMC of HIV-1-infected donors. Half of the PBMC were stimulated with phytohemagglutinin (2 μg/ml) for 24 h and then pulsed with corresponding peptides at 100 μM for 1 h and irradiated before being added to the other half of the PBMC. A total of 3×10^6 cells in each well of a 96-well U-bottom plate, with at least 10 wells for each sample, were cultured in R10; 10% Lymphocult T (Biotest, Dreieich, Germany) was added to the medium on day 3 of culture. The CTL lines were maintained by adding fresh R10 medium containing 10% Lymphocult T every 3 to 4 days and splitting the well accordingly. Assays were performed on day 14 to 28 of culture.

Synthetic peptides. Peptides were manufactured at the Takara Shuzo Co., Ltd. (Shiga, Japan). The purity of peptides was >99% as determined by high-pressure liquid chromatography, and the identity of peptides was confirmed by matrix-assisted laser desorption ionization–mass spectrometry. Lyophilized peptides were dissolved in dimethyl sulfoxide and diluted in phosphate-buffered saline to make a stock concentration (2 mM). Further dilution was made in RPMI 1640 to make working concentrations of 200 μM for the induction of CTLs and of 20 μM for the preparation of target cells.

^{51}Cr release assay. In 96-well U-bottom plates, target cells were divided into aliquots at 5,000 per well. Effector cells were added to target cells at different effector/target (E:T) ratios. The amount of ^{51}Cr release in the culture supernatants was quantified after 6 h of incubation, and the percent specific lysis was determined by using the following formula: $[(E - M)/(D - M)] \times 100$, where E is the experimental ^{51}Cr release, M is the ^{51}Cr released in the presence of culture medium (which ranged between 15 and 25% of total release), and D is the total ^{51}Cr released in the presence of 5% Triton X-100 detergent. The results were regarded as positive when recognition of the HIV target was >10% above the control. The SD_{50} is the peptide concentration giving 50% of maximal specific lysis of target cells pulsed with 10 μM synthetic peptide (28).

Replication kinetics assay. Subconfluent 293T cells in Falcon 25-cm^2 T flasks (Becton Dickinson) were transfected by lipofection (Roche Molecular Biochemicals), with 2 μg of HXB2ev replication-competent HIV-1 plasmids, in which various mutations were introduced. After 60 h of culture, the supernatant was harvested, filtered through a 0.45-μm-pore-size filter, and used as mutant virus stocks. Two million Jurkat cells or eight million H9 cells were infected with an equivalent of 40 ng of p24 antigen of mutant viruses in 2 ml of R10 for 1 h. Cells were washed three times with 10 ml of R10, resuspended with 5 ml of R10, and cultured in a 12.5-cm^2 T flask at 37°C in 5% CO_2. Every 2 or 3 days, 1.5 ml of supernatant was harvested and replaced with fresh R10. The concentration of p24 was measured by using a p24 ELISA kit (Zeptometrix Corp.).

This study was approved by the Ethics Committee of the University of Tokyo.

RESULTS

Full-length *gag* clones of field isolates. We used 6 of 13 full-length *gag* clones that were isolated from the five infected individuals (Fig. 2). All of the clones did not have any stop codons. In the present study, we focused on the processing and presentation of three CTL epitopes: the HLA-A*0201-restricted epitope SLYNTVATL, the A24-restricted epitope KYKLKHIVW in p17 matrix protein (MA), and the HLA-B*5101-restricted epitope NANPDCKTI in p24 capsid protein (CA) (11, 26, 27). Amino acid sequences within the three epitope regions and the N- and C-terminal 15-amino-acid residues flanking each epitope were analyzed; the six clones were selected to maximize the diversity of amino acid sequences in the epitopes and its flanking regions.

The A*0201-restricted epitope and its flanking regions were highly variable. However, we did not observe a previously recognized variation in the flanking region, Arg (R) to Lys (K) at position 76 in our clones (4). In contrast, the B*5101-restricted epitope and its flanking regions were conserved except for clones IMS2-5 and IMS4-24. In the A24-restricted epitope and its flanking regions, variations were seen almost exclusively within the epitope region with two exceptions, a Lys (K)-to-Ser (S) mutation at position 26 (K26S) in clone IMS4-24 and an Arg (R)-to-Lys (K) at position 15 in clone IMS2-5. The Lys (K)-to-Arg (R) mutation at position 30 within the A24-restricted epitope was seen more frequently than any other sequences; none of the 13 clones had the wild-type sequence of KYKLKHIVW. We incorporated the six *gag* clones into the HIV-1 vector with *env* and *nef* deleted, pCTLpac (Fig. 1), to make target cells expressing *gag* genes of these filed isolates.

CTL recognition of target cells endogenously expressing *gag* genes of clinical isolates. We generated A*0201-restricted SLYNTVATL (wild type) epitope-specific oligoclonal CTL lines from one HIV-1-infected individual (IMS1) with A*0201 and used the lines to test the killing of the six different *gag* clones expressed on A*0201-matched B-LCLs by a conventional ^{51}Cr release assay. The A*0201-restricted CTLs efficiently recognized target cells expressing *gag* clones IMS1-29, IMS1-28, and IMS6-34, which encode either wild type or the SLYNTIATL sequence in the CTL epitope region. In contrast, the same CTLs did not recognize cells expressing *gag* clones IMS2-5, IMS4-24, and IMS7-11, which encode SLYNLVATL, SLFNTVAVL, and SVYNTVATL, respectively, indicating that these clones escaped from A*0201-restricted CTL recognition (Fig. 3a).

CTL recognition of IMS1-29 and IMS6-34 was also tested with recombinant vaccinia viruses expressing the *gag* gene of these variants in parallel with the VSV-G-pseudotyped HIV-1 vectors. The HIV-1 vector method demonstrated the CTL killing as well or slightly better than the vaccinia method did (Fig. 3b).

We used three B*5101-restricted NANPDCKTI -specific CTL clones to test the CTL recognition of five representative *gag* clones. The CTL clones recognized four *gag* clones, which convey the wild-type B*5101-restricted epitope sequence; they also recognized IMS2-5 that had a substitution in the flanking region. None of the clones recognized the IMS4-24 clone, which had the variant sequence NSNPDCKNI in the epitope region (Fig. 3c).

A24-restricted KYKLKHIVW (wild type) specific-CTL lines did not recognize synthetic peptides of the most common sequence, KYRLKHIVW (3R mutant type), and the other variant, RYRLKHIVW (Fig. 3d). These two variants were shown to bind to the A*2402 MHC class I molecule in a binding assay (data not shown). We screened eight A24-positive individuals for the presence of CTL activities against the 3R mutant epitopes and found one individual who carried CTLs recognizing the 3R mutant peptide. A24-restricted 3R mutant-reactive CTL lines were induced from this A24-positive individual and used for the remaining experiments. The 3R mutant-reactive CTL lines recognized target cells expressing IMS1-29 and IMS4-24 *gag* clones, both of which carry the 3R mutant sequence, but did not recognize any